ISSN 1068-3755, Surface Engineering and Applied Electrochemistry, 2019, Vol. 55, No. 2, pp. 138–149. © Allerton Press, Inc., 2019.
Russian Text © F.I. Danilov, A.A. Kityk, D.A. Shaiderov, D.A. Bogdanov, S.A. Korniy, V.S. Protsenko, 2018, published in Elektronnaya Obrabotka Materialov, 2018, No. 3, pp. 21–33.

Electrodeposition of Ni–TiO_2 Composite Coatings Using Electrolyte Based on a Deep Eutectic Solvent[1]

F. I. Danilov[a], A. A. Kityk[a], D. A. Shaiderov[a], D. A. Bogdanov[a], S. A. Korniy[a, b], and V. S. Protsenko[a, *]

[a] *Ukrainian State University of Chemical Technology, Dnipro, 49005 Ukraine*

[b] *Karpenko Physico-Mechanical Institute of the NAS of Ukraine, Lviv, 79060 Ukraine*

**e-mail: Vprotsenko7@gmail.com*

Received March 16, 2018; revised April 17, 2018; accepted April 17, 2018

Abstract—Deep eutectic solvents are nowadays considered to be very promising analogues of room temperature ionic liquids. They can make a significant contribution to the development of novel efficient, economic and environmentally friendly processes, particularly, in surface engineering and electroplating. The electrodeposition of Ni–TiO_2 composite coatings from an electrolyte based on a deep eutectic solvent, ethaline, was studied in this work. Titania particles were introduced into the plating bath in the form of Degussa P 25 nanopowder. The content of titania in electrodeposited composite coatings was shown to depend on the stirring rate, current density and TiO_2 concentration in the electrolyte and can reach ca. 2.35 wt %. The microstructure and the surface morphology of the obtained composite layers were characterized. The formation of nanocrystalline nickel matrix was detected. The introduction of TiO_2 particles into nickel-based coatings resulted in an increase in the microhardness of deposits. The data obtained via the electrochemical impedance spectra technique revealed an improvement in the corrosion resistance of coatings due to titania particles incorporation into deposits. The Ni–TiO_2 composite coatings manifested a photocatalytic activity towards the reaction of photochemical degradation of methylene blue organic dye in water solution.

Keywords: electrodeposition, nickel, titania, composite coating, deep eutectic solvent

DOI: 10.3103/S106837551902008X

INTRODUCTION

Electrochemical deposition of composite coatings is known to provide the fabrication of finishing layers with enhanced microhardness, high wear, and corrosion resistance and allows imparting various useful physicochemical and service properties to the surfaces [1, 2]. Electrodeposited composite coatings are composed of a metallic matrix and a dispersed phase of nano- or micro-sized particles entrapped into the metallic matrix during electrodeposition. Although various metals can be used as a matrix in electrodeposited composite coatings, nickel seems to be especially widely used for the electrochemical synthesis of composite layers [1, 3–17].

Among a large number of different kinds of dispersed particles which can be co-deposited with the Ni matrix, titania occupies a special place. This is due to the fact that titania is a versatile and available material that has a wide variety of applications: from paint and cosmetics to photocatalysts, electrocatalysts, hydrogen production, storage batteries, fuel cells, solar cells, sensors, and various environmental and biological/health-related applications [18].

Numerous studies showed that the introduction of TiO_2 dispersed particles into the nickel matrix results in a substantial improvement in the mechanical and physicochemical properties of coatings [9–15]. The mechanical properties of the electrodeposited Ni–TiO_2 nanocomposite films (microhardness and sliding wear resistance) were shown to be superior to those of the nickel matrix [9]. The improvement in microhardness, wear resistance and corrosion resistance resulted from the introduction of titania nanoparticles into the Ni electrodeposited layers, was also confirmed elsewhere [10, 11]. The composite Ni–TiO_2 coatings manifest both photo-induced hydrophility and photocatalytic activity, which determines their self-cleaning character [12]. The Ni–TiO_2/TiO_2 composite multilayers, electrodeposited from a nickel Watts bath containing a TiO_2 sol, showed appreciable photocatalytic and photoelectrocatalytic activities towards the degradation of methyl orange dye and the decomposition of phenol, respectively [13]. The co-deposited Ni–TiO_2 nanocomposite coatings can also be used for fuel cell applications, in particular, in the electro-oxidation of methanol [14]. An increase in the corrosion resistance and the passivation tendency of the nickel matrix due to TiO_2 particles incorporation has been reported in [15].

[1] The article was translated by the authors.

Commonly, the electrodeposition of composite coatings is performed using aqueous electrochemical systems [1–3, 5–15]. Although aqueous colloidal electrolytes are relatively simple, cheap and available, they have a number of drawbacks. For instance, the processes of aggregation of the dispersed phase (coagulation and flocculation) can quickly occur in water solutions [19–21], which results in the phase separation (sedimentation) and deterioration of the properties of the obtained composites.

Recently, an alternative to "usual" aqueous plating baths has been developed; it involves the application of deep eutectic solvents (DESs) [22–25]. DESs consist of a eutectic mixture of some organic and inorganic compounds having a melting point significantly lower than that of each individual component [23–25]. DESs are now considered to be a new and promising type of ionic liquids that can be used in various fields of application, particularly, in electrochemistry and electroplating [22, 23]. DESs are regarded as promising solvents in metal deposition processes due to their excellent properties, such as wide electrochemical potential windows, a high solubility of metal salts, a relatively high conductivity, a negligible vapor pressure, they are easily accessible and environmentally safe [23].

A number of papers reported the use of DES-based electrolytes in electrodeposition of composite coatings [4, 26–30]. For example, the authors in [26] described the electrodeposition of silver/SiC and silver/Al_2O_3 composites from the electrolyte containing an ethylene glycol/choline chloride based DES. High dispersed-phase loadings can be achieved and these have significantly improved properties compared with the pure metal.

The electrodeposition of Ni/SiO_2 nanocomposites from deep eutectic solvents was also investigated [4, 27]. The application of DES based electrolytes effectively reduces the agglomeration of nanoparticles in the plating bath and ensures a uniform distribution of nanoparticles within a metal matrix. The Ni/SiO_2 nanocomposites with good tribological properties and enhanced corrosion resistance can be fabricated.

The effects of the particle content in the electroplating bath on the basis of DES, current density and stirring rate on the content of micro or nano-sized SiC particles incorporated into the Ni matrix were investigated [28]. The microhardness and wear resistance of Ni–SiC composite coatings were significantly better that those of the Ni matrix.

To the best of the authors' knowledge, the preparation and characterization of Ni–TiO_2 electrodeposited composites from DES based electrolytes have not been reported yet. Therefore, this work was aimed to study the electrodeposition of nickel–titania composite films from an electrolyte based on DES.

The effect of electrolysis conditions on the TiO_2 content in the coatings was determined and analyzed. The surface morphology and the microstructure of the deposits obtained were studied. The microhardness values of Ni–TiO_2 electrodeposited composites were measured. The effects of the TiO_2 content on the corrosion resistance and photocatalytic performance of nickel–titania composites were investigated and discussed.

EXPERIMENTAL

Preparation of DES-Based Electrolyte and Electrodeposition of Composite Coatings

In this work, a nickel electroplating bath was used based on a deep eutectic solvent commercially known as ethaline [22, 31, 32]. This DES is composed of the eutectic mixture of choline chloride and ethylene glycol in a molar ratio of 1:2.

Choline chloride (Aldrich, purity >98%) was recrystallized from isopropanol, filtered and then dried under vacuum. Ethylene glycol (Aldrich, purity >99%) and $NiCl_2 \cdot 6H_2O$ (Aldrich, purity >99%) were used as received. Ethaline was prepared by mixing choline chloride and ethylene glycol in the above eutectic molar ratio. The mixture was thermostatted at 70°C and stirred until a homogenous, colorless liquid formed. Then $NiCl_2 \cdot 6H_2O$ salt was added to the prepared DES and the mixture was stirred at 70°C to form a green homogenous liquid. The content of Ni(II) was 1 mol dm^{-3}.

The TiO_2 nano-powder (Degussa P 25, Evonik), with an average particle size of 25–30 nm, was used without any pretreatment. To obtain a colloidal electrolyte for composites electrodeposition, a weighed portion of the TiO_2 Degussa P 25 nano-powder was introduced directly into the electroplating bath, the concentration of TiO_2 in the bath being 1, 2, 5, 10 or 15 g dm^{-3}. Immediately after that the electrolyte was stirred for 1 h by a mechanical agitator and then ultrasonically treated with a UZDN–A ultrasonic disperser for 1 h (22.4 kHz, 340 W dm^{-3}) to reach a uniform distribution of colloidal particles in the plating bath.

A gold plate ($S = 3.54$ cm^2) fixed in a plastic holder was used as a substrate for composites electrodeposition. Prior to each experiment, the surface of the gold electrode was treated with magnesium oxide, etched for several minutes in 1:1 (vol.) HCl solution and then thoroughly rinsed with double distilled water. The electrolysis was carried out with nickel anodes. The electrodeposition of the Ni–TiO_2 composite coatings was performed under the conditions of a continuous bath agitation with a magnetic stirrer, the stirring rate was varied from 300 to 800 rpm. The electrodeposition was conducted at a steady current density in a usual thermostatted glass cell (25°C). The cathodic current density was changed in the range of 1 to 15 mA cm^{-2}.

The electrolysis duration has been adjusted so that the deposits with a thickness of about 20 μm were obtained. It should be noted that the rate of electrodeposition and the composition of the coatings practically do not depend on the electrolysis duration.

Characterization of Electrodeposits

The surface morphology of the composite coatings was studied by the scanning electron microscopy (SEM) (Zeiss EVO 40XVP) in secondary electron regimes. The chemical composition of the surface layers was determined by the energy dispersive X-ray spectroscope coupled with a SEM microscope (Oxford INCA Energy 350).

The bulk composition of the Ni–TiO_2 composite coatings was determined by the X-ray fluorescence analysis.

The X-ray diffraction analysis (XRD) was performed by an XRD spectrometer DRON–3.0 in the monochromatized CoK_α radiation. The crystalline size was estimated by the Scherrer equation:

$$D = \frac{K\lambda}{\beta\cos\theta}\frac{180^\circ}{\pi}, \quad (1)$$

where D is the average crystalline size, λ is the wavelength of X-rays (1.78901 Å), K is a constant (usually evaluated as 0.94), β is the corrected peak width at a half-maximum intensity in degrees and θ is the scattering angle.

Vickers microhardness (HV) was measured by means of PMT–3 apparatus at a 100 g load. The average value of the coatings microhardness was calculated as an average of five separate measurements.

The study of corrosion resistance of the synthesized composite coatings was carried out by means of electrochemical impedance spectra (EIS) techniques in the 3% NaCl aqueous solution as a corrosive medium at 25°C. Plates made of mild steel were used as substrates for coatings electrodeposition in this series of experiments. The thickness of deposits was ca. 20 μm.

Electrochemical impedance was measured using a Potentiostat/Galvanostat Reference 3000 (Gamry). A common thermostatted glass three-electrode cell was used; the electrode compartments being separated by a glass porous diaphragm. Dissolved atmospheric oxygen was removed by purging purified electrolytic hydrogen. The counter electrode was porous graphite, its surface area considerably exceeded the overall surface area of the working electrode. The electrode potentials were measured with respect to the saturated Ag/AgCl-electrode and recalculated to the scale of a standard hydrogen electrode. Electrochemical impedance spectra were recorded at open circuit potentials in a frequency range of 0.01 Hz to 100 kHz, with a constant AC voltage amplitude of 5 mV. The data of EIS were treated (that means the development of electrical equivalent circuits and the determination of quantitative parameters of their elements) using Gamry Elchem Analyst software package.

The photocatalytic properties of the Ni–TiO_2 composite deposits were tested in an in-house fabricated reactor, which was described in detail elsewhere [33]. The coatings with a thickness of about 20 μm were electrodeposited on mild steel plates. Methylene blue (MB) was used as a test organic dye. Its photochemical degradation was estimated in aqueous solutions under the action of the UV irradiation with an effective spectral range of 180–275 nm. The decolorization kinetics was studied within 105 min at the temperature of 25°C. The content of MB dye in the solution was determined from its absorbance change at a wavelength of 670 nm.

RESULTS AND DISCUSSION

Effects of Electrodeposition Parameters on TiO_2 Content in Composite Coatings

It is known that hydrodynamic conditions have strong influence on the composition of electrodeposited composite coatings [1, 6]. On the one hand, the intensity of electrolyte stirring governs the rate at which colloidal particles are being brought to the electrode surface [34]. On the other hand, the electrolyte stirring during the electrodeposition of composite films is required to ensure good distribution uniformity of the particles in the plating bath [1].

As follows from Fig. 1, the TiO_2 content in composite films increases with an increase in the stirring rate when the stirring rate is lower than a certain threshold value. Once the velocity of stirring exceeds this threshold value, the content of TiO_2 in composites begins to diminish.

This behavior can be explained on the base of the conception developed in [35]. Those authors found that for a constant current density there are two convection regimes. At relatively low velocities of stirring, intensifying the convective flow leads to more particles being incorporated into deposits. However, at a relatively high stirring rate, the incorporation tends to decrease due to ejecting loosely attached particles by an intensive radial flow. This clarifies the appearance of the threshold value of the stirring rate at which the particles content in composite coatings reaches a maximum (ca. 500 rpm for Ni–TiO_2 electrodeposits under consideration). To ensure an enhanced titania content in coatings, all further experiments were conducted at a stirring rate of 500 rpm.

The effect of the cathode current density on the composition of Ni–TiO_2 composite coatings obtained from the DES-based plating bath is shown in Fig. 2. When increasing the current density from 1 mA cm^{-2} to 10 mA cm^{-2}, a gradual increase in the TiO_2 content in composite films is observed. At a further growth of

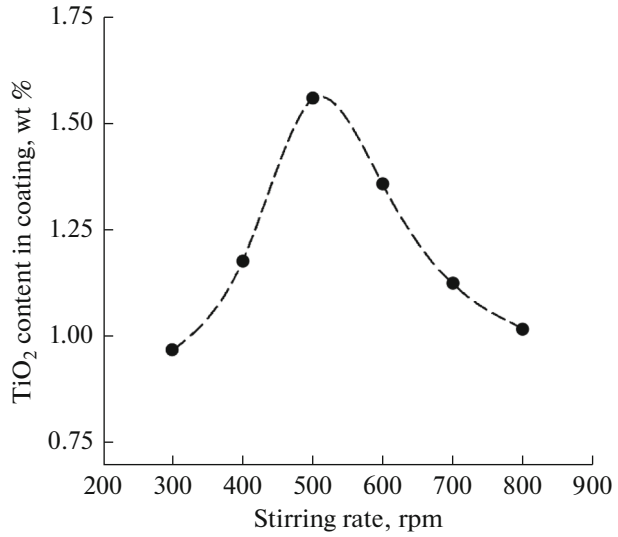

Fig. 1. Effect of stirring rate on TiO_2 content in the composites electrodeposited at current density of 10 mA cm^{-2} and titania concentration in the electrolyte of 1 g dm^{-3}.

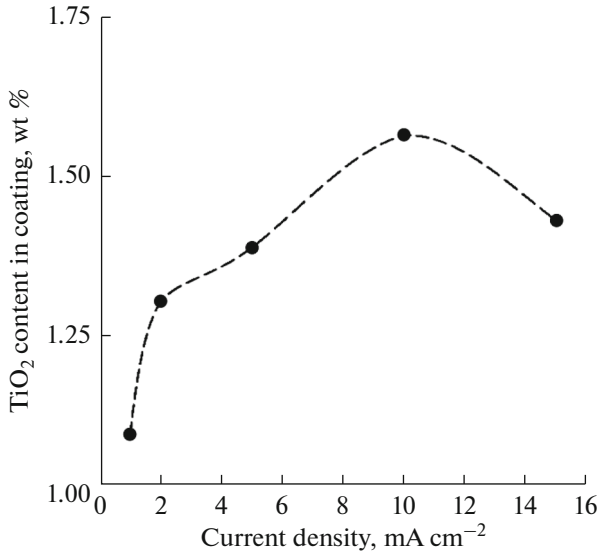

Fig. 2. Effect of current density on TiO_2 content in the composites electrodeposited at stirring rate of 500 rpm and titania concentration in the electrolyte of 1 g dm^{-3}.

the current density (up to 15 mA cm^{-2}), the content of TiO_2 coatings slightly diminishes. In general, the change of the titania content in composites with the current density is relatively weak.

Many researchers have found that modest increases in the current density lead to a higher particle incorporation in the deposit but behavior can be more complex [2]. In some cases a clear maximum is seen in the particle content of the composite electrodeposits if some threshold current density range is traversed.

The authors in [28] also detected a maximum of the dependence of the SiC particles content in coatings on the current density for the electrodeposition of Ni–SiC composites from a deep eutectic solvent. It was suggested that at lower current densities a relatively slow reduction rate of Ni(II) allows the particles to have plenty of time to adsorb on the electrode surface, which favors the particles incorporation. A further increase in the current density (which means a higher rate of metallic matrix growing) impedes attaching the particles and, as a consequence, the content of inert particles in coatings decreases. Such interpretation can also explain the data obtained in the present work.

In all subsequent experiments, nickel–titania composite coatings have been deposited at a constant current density of 10 mA cm^{-2}.

Figure 3 shows the effect of the concentration of the TiO_2 nano-powder in the plating bath on the titania content in the electrodeposited composites. A gradual increase in the content of titania particles in coatings is observed with increasing the concentration of TiO_2 in the colloidal electrolyte.

According to Guglielmi's model of composite electrodeposition [36], the particles inclusion into a metallic matrix occurs in two consecutive steps of adsorption. In the first step ("loose adsorption"), the particles are reversibly adsorbed on the electrode surface and yield a high degree of coverage. In the second step, the reduction of metal ions adsorbed on the particles creates the circumstances of an irreversible adsorption ("strong adsorption"). Further, the particles are engulfed by the growing of the metallic matrix. Evidently, the adsorption rate of TiO_2 particles should

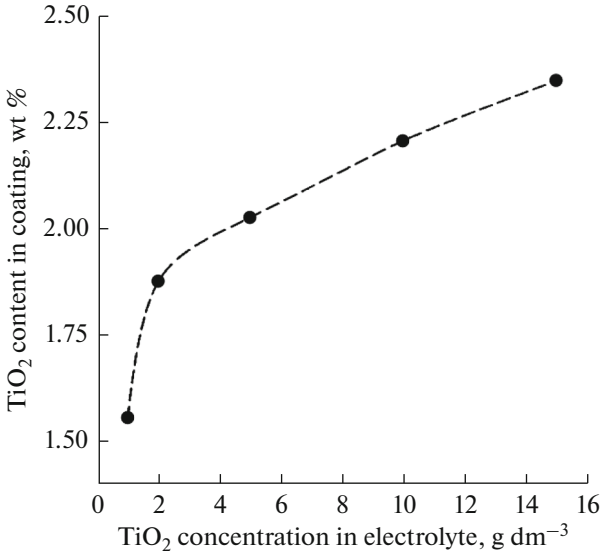

Fig. 3. Effect of titania concentration in the plating bath on TiO_2 content in composites electrodeposited at stirring rate of 500 rpm and current density of 10 mA cm^{-2}.

increase with the particles concentration in the colloidal electrolyte, resulting in a growth of the particle content in composite coatings.

Comparing the data obtained in the present work with those reported earlier [9–12, 14], it is essential to note that the content of TiO_2 particles embedded into the nickel matrix from a DES based plating bath is relatively low: it reaches only 2.35 wt % (at 15 g dm^{-3} TiO_2 in the electrolyte, see Fig. 3). At the same time, the maximal amount of the particles incorporation varied between 3.26 and 11.58 wt % TiO_2 when Ni–TiO_2 composite layers were electrodeposited from "common" aqueous baths, depending on the electrolyte type, the composition and electrolysis conditions [9–12, 14, 15]. A following possible explanation for this observation can be given.

Each particle suspended in a plating bath is covered by a thin layer of the electrolyte which must be shed to be embedded into the growing metal deposit. Similarly, a thin layer of electrolyte components should be removed from the electrode surface in the course of the entrapment of particles into the depositing matrix. This also includes a possible presence of some adsorbed layers on the electrode that must be partially or fully broken.

DES-containing electrolytes differ from aqueous ones by considerably higher viscosity and density [23]. Evidently, DES-based systems require appreciably more time and energy to destroy dense and viscous films formed on the surfaces of both particles and a growing metal matrix, which hinders the rate of the particles inclusion into deposits, and hence reduces a maximum available content of an inert dispersed phase in the synthesized composite coatings.

It should be stressed that a DES-containing plating bath under study exhibits excellent dispersion stability. No visible sign of coagulation and sedimentation, even after ceasing electrolyte stirring (at least, during one week of observations), was detected.

SEM Investigation of Surface Morphology

The effect of the TiO_2 Degussa P 25 particles introduction into the nickel matrix on the surface morphology of coatings deposited from ethaline containing plating bath can be seen in Fig. 4. SEM images of pure Ni coatings exhibited a relatively even surface with a nodular structure, with an average diameter of nodules about 0.5–2 μm (Fig. 4a). There are a small number of defects (small protrusions) on the surface, however, cracks are not observed. The energy dispersive X-ray spectroscopy revealed that the surface of "pure" nickel coatings chiefly consisted of Ni, the presence of small amount of such elements as O, C and Cl was detected too.

When a small amount of the TiO_2 nano-powder (1–5 g dm^{-3}) was added to the electrolyte, a great number of spherical nodules of 2–10 μm appeared on the surface (Figs. 4b–4d). The presence of Ni, Ti, O, C and Cl on the surface was observed in the EDX spectra of the Ni–TiO_2 composite coating (not shown). Trace amounts of oxygen, carbon and chlorine can be associated with the inclusion of some components of the electrolyte which are adsorbed on the electrode surface.

It is interesting that the surface structure became more uniform and finer when the concentration of TiO_2 reached 10 g dm^{-3} (Fig. 4e). However, a further increase in the TiO_2 concentration in the plating bath resulted in the coarsening of the surface structure and relatively large spheroidal protrusions appeared again (Fig. 4f).

Thus, the obtained results allow supposing that TiO_2 nanoparticles suspended in the DES-based electrolyte and embedded into the nickel matrix affect the processes of nucleation/growth and the formation of metal crystallites; thereby, TiO_2 nanoparticles act as peculiar surface-active agents. It is well-known that the surfactants, when added to the metal plating baths, adsorb on the growing surface, ensure leveling the surface profile and cause the formation of fine-crystalline deposits. In our case, at higher titania particles concentration, their beneficial effect on surface smoothing is enhanced and the finest surface morphology is observed at the TiO_2 content in the baths of 10 g dm^{-3} (Fig. 4e). A further growth of TiO_2 particle concentration in the electrolyte (up to 15 g dm^{-3}) may result in partial agglomeration of particles in the electrolyte. The embedding of larger particles into metal deposits promotes the coarsening of crystallites (Fig. 4f).

It should be noted that the effect of the inert particles co-deposition on the nucleation/growth mechanism was earlier observed in the case of electrodeposition of Ni–SiC composite coatings from deep eutectic solvents [28].

XRD Investigation of Coatings Structure

The typical XRD patterns of pure Ni and Ni–TiO_2 composite coatings deposited from a DES containing electrolyte are shown in Fig. 5. The reflections of the face centered cubic nickel and anatase TiO_2 planes were detected. Due to a small amount of TiO_2 in coatings, the corresponding reflections from the anatase phase were very weak; they could be seen quite well on XRD patterns only for samples obtained from the plating baths with the highest content of TiO_2 particles (10 and 15 g dm^{-3}).

Broad half-width values of the XRD profile of Ni indicate the nanocrystalline structure of the metallic matrix. The average crystalline sizes of the deposits were calculated based on the full width at half maximum of X-ray peaks of diffraction using Eq. (1) for (111) plane corresponding to the diffraction peaks with the highest intensity. The calculated values of D are

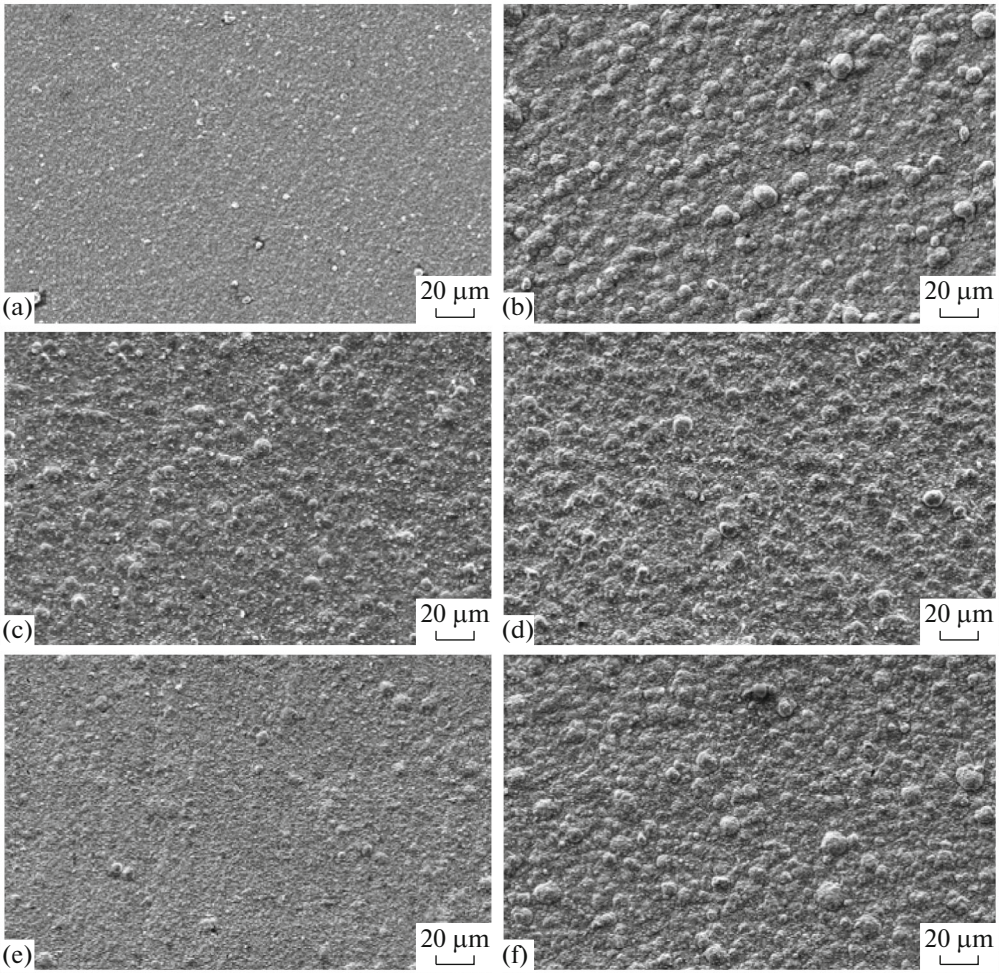

Fig. 4. SEM images of: (a) pure nickel and (b–f) Ni–TiO_2 composite coatings electrodeposited at different titania particles content in the plating bath (g dm^{-3}): (b) 1, (c) 2, (d) 5, (e) 10, and (f) 15. All coatings were electrodeposited at stirring rate of 500 rpm and current density of 10 mA cm^{-2}.

summarized in Table 1. It is seen that the values of the crystalline size vary in a relatively narrow range of ca. 9–14 nm. Although there is no marked trend, the lowest crystalline size is achieved for coatings obtained from the bath with the TiO_2 concentration of 10 g dm^{-3}, when the most uniform surface morphology is observed. Thus, there is a certain correlation between the crystalline size determined by the Scherrer equation and the grain size evaluated via SEM images.

Table 1. Calculated values of crystalline size of coatings deposited from DES-based electrolyte at stirring rate of 500 rpm, current density of 10 mA cm^{-2} and different TiO_2 concentration in a plating bath

Concentration of TiO_2 in a plating bath, g dm^{-3}	D, nm
0	12.6
1	13.4
2	13.3
5	11.8
10	9.9
15	13.9

Microhardness of Coatings

Figure 6 shows the relationship between the content of TiO_2 particles in a nickel plating bath and the microhardness of the electrodeposited coatings. An introduction of titania particles into the nickel matrix and an increase of their content result in an increase of the deposits microhardness.

The strengthening of composite electrodeposits is commonly attributed to two mechanisms: the grain refinement strengthening from the Hall–Petch relationship and the dispersion strengthening due to the

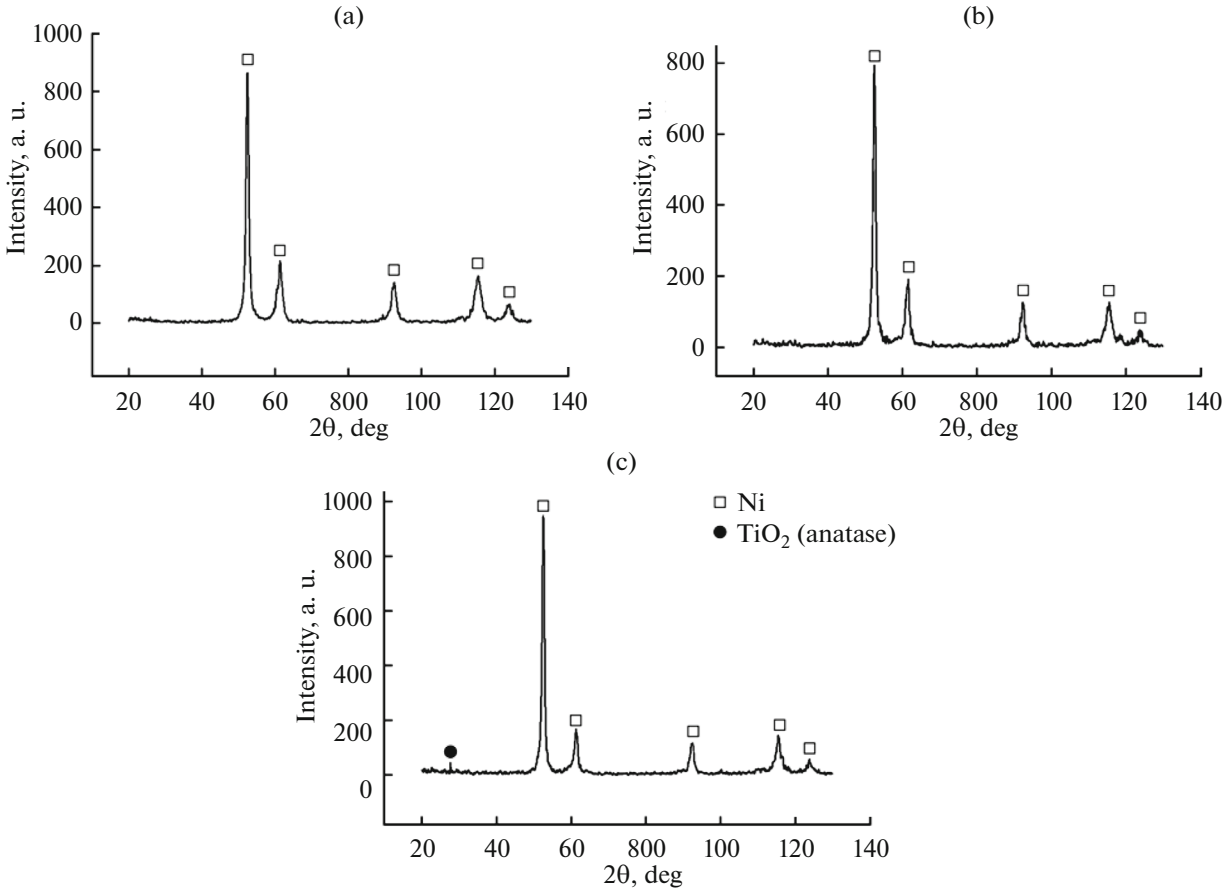

Fig. 5. Typical XRD patterns of: (a) Ni and (b, c) Ni–TiO_2 composite coatings electrodeposited from the DES-based electrolyte at stirring rate of 500 rpm, current density of 10 mA cm^{-2} and different TiO_2 nano-powder concentration (g dm^{-3}): (a) 0, (b) 1, and (c) 15.

Orowan mechanism [37]. The Hall–Petch equation suggests that the microhardness of a nano-sized material increases when diminishing the grain size. As shown above (Table 1), there is no appreciable decrease in the grain size when the content of TiO_2 in the plating bath increases. Therefore, it is assumed that an increase in microhardness of Ni–TiO_2 composites prepared using DES-based electrolytes is chiefly governed by the Orowan mechanism. This phenomenon is attributed to dispersion of fine colloidal particles, which impedes the motion of dislocations in the metallic matrix resulting in an increase in the material hardness [21, 37]. It is clear that an increase in the concentration of closely spaced dispersed particles entrapped into the coating leads to an increase in the number of obstacles to moving the dislocations. This ensures more pronounced dispersion strengthening.

However, at the highest content of TiO_2 in the electrolyte (15 g dm^{-3}), an appreciable decrease of microhardness is observed in spite of a further increase of the titania content in coatings. It is supposed that the

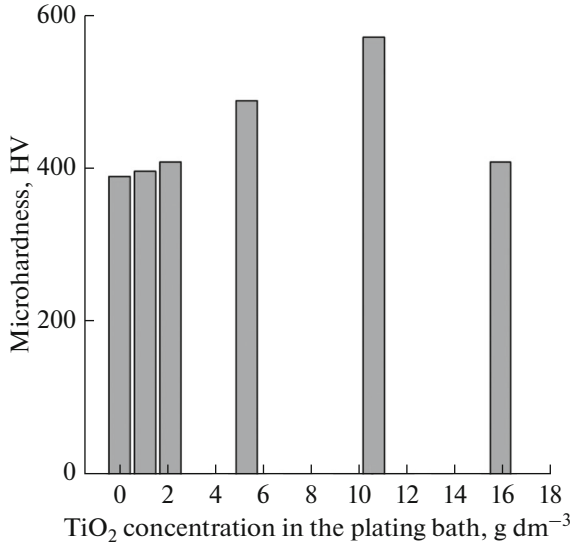

Fig. 6. Microhardness of coatings expressed as function of TiO_2 concentration in the plating bath. The coatings are deposited at stirring rate of 500 rpm and current density of 10 mA cm^{-2}.

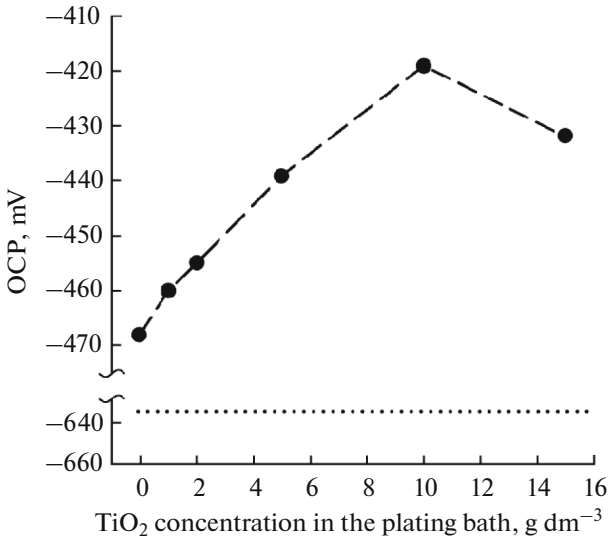

Fig. 7. Relationship between TiO_2 content in the plating bath and OCP of electrodeposited coatings immersed in 3% NaCl solution. The coatings are deposited at stirring rate of 500 rpm and current density of 10 mA cm^{-2}. The dotted line depicts the OCP of the steel substrate without any coating.

reduction of microhardness is due to the coarsening of the surface grains which is revealed by SEM study (Fig. 4f): more defective and less uniform surface morphology causes diminishing the surface strength of the material.

EIS Study of Corrosion Behavior

Figure 7 shows the relationship between the open circuit potential (OCP) of coatings immersed in an aggressive environment containing 3% NaCl and the TiO_2 concentration in the elecroplating bath. It should be noted that the values of the OCP manifest only minute changes with time after immersion of the samples in a corrosive medium (the deviations are less than ±(25...30) mV within two hours of observations). Hence, the measured OCP values reflect, in fact, a steady-state condition.

It is clearly seen that the introduction of TiO_2 particles into the nickel matrix and an increase of their content shift the corrosion potential to nobler values indicating an enhancement of the corrosion stability of coatings. However, when the TiO_2 concentration reaches 15 g dm^{-3}, the OCP value reduces slightly.

To get detailed information about the influence of embedding the TiO_2 Degussa P 25 particles into the nickel matrix upon the corrosion resistance of coatings, the electrochemical impedance spectroscopy was used. The measurements of impedance spectra were performed at the OCPs. Several typical Nyquist diagrams of deposits plated from the DES-based nickel plating bath are shown in Fig. 8.

All obtained Nyquist diagrams look very similar: the impedance plots exhibit depressed semicircles, which implies that the electrochemical process is controlled by the charge transfer step and occurs on the inhomogeneous electrode surface. This behavior can be described by the so-called constant phase element (CPE) [38]. Figure 9 shows an equivalent circuit adapted for the interpretation and analysis of experimental impedance data. The electrical equivalent circuit contains polarization resistance of the electrochemical reaction (R_{ct}), the constant phase element (CPE) which characterizes the interface of "solid electrode/solution", and the ohmic resistance of the solution (R_s).

As concerns the impedance of the CPE, it can be given by the following formula [39]:

$$Z_{CPE} = \left[Q(j\omega)^n\right]^{-1}, \quad (2)$$

where Q is a constant; $j = \sqrt{-1}$ is the imaginary unit; ω is the angular frequency of alternating current; and n is the dimensionless empirical exponent corresponding to phase deviation and associated with inhomogeneity of the electrode surface.

The experimental data in Fig. 8 are displayed as symbols and the continuous lines are obtained by curves fitting using the electrical equivalent circuit shown in Fig. 9. The calculated kinetic parameters are summarized in Table 2. For the sake of comparison, the impedance characteristics of the corrosion of a steel substrate without any coatings are also given.

The polarization resistance of the electrochemical reaction, R_{ct}, can be considered as a parameter which explicitly characterizes the corrosion stability of coatings. It follows from the obtained results that R_{ct} increases with the TiO_2 content in the electrolyte and hence in composite coatings, which indicates an improvement in the corrosion stability. However, this uniform dependence is violated when the titania content in the bath reaches 15 g dm^{-3}: a certain decrease of R_{ct} is observed at this TiO_2 concentration. Thus, the most corrosion-resistant coatings are electrodeposited from the plating bath containing a threshold value of TiO_2 concentration (ca. 10 g dm^{-3}).

As concerns the empirical exponent n in Eq. (2), it characterizes the extent of inhomogeneity of the electrode surface rather than the extent of surface roughness (a real surface area). Our findings show that the most inhomogeneous surface is formed at the abovementioned threshold value of the TiO_2 concentration in the plating bath. This corresponds to a large amount of nanoparticles finely dispersed in the metallic matrix providing the formation of a highly corrosion-resistance material. Both an increase and a decrease in the TiO_2 concentration result in an increase in the value of n.

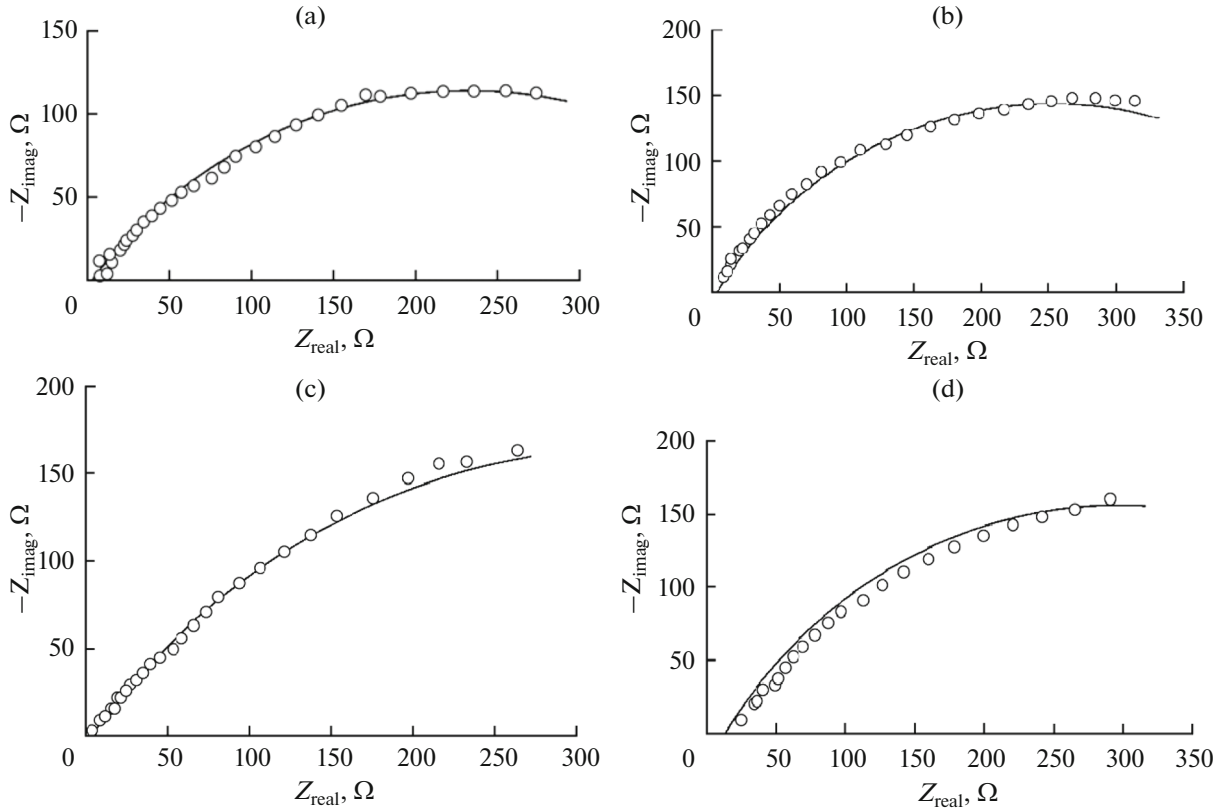

Fig. 8. Typical Nyquist plots of Ni and Ni–TiO_2 composite coatings deposited from the DES based plating bath at stirring rate of 500 rpm, current density of 10 mA cm^{-2}, and different TiO_2 contents in the electrolyte (g dm^{-3}): (a) 0, (b) 2, (c) 10, and (d) 15. The measurements were conducted at OCP in 3% NaCl solution. The visible electrode surface was 2 cm^2. The symbols denote the measured (experimental) impedance spectra and solid lines represent fitted results.

The Q values in Eq. (2) are often associated with the surface area available for the electrochemical reaction [19]. Comparing the Q values for nickel and nickel–titania composites deposited from DES-based baths, one can conclude that the highest values of Q correspond to the lowest empirical constants n.

In general, the obtained data show that the inclusion of titania nanoparticles in an electrodeposited metallic matrix leads to an enhancement of the corrosion stability of composite coatings as compared with pure nickel. It is assumed that the improvement in corrosion resistance is due not only to the formation of a protective physical barrier, which partially blocks the electrode surface and is composed of "inert" TiO_2 particles, but also to the formation of corrosion micro-cells in which TiO_2 acts as cathode and nickel as anode [40].

Photocatalytic Activity of Ni–TiO_2 Composite Coatings

Nowadays the use of heterogeneous photocatalysis (TiO_2/UV) in the treatment of wastewaters attracts considerable attention [41]. In this context, the search for convenient and efficient supporting materials to anchor the TiO_2 catalyst remains an important challenge in advanced oxidation processes based on titania photocatalyst [42]. It is believed that the electrodeposition of composite coatings with dispersed TiO_2 particles is a very promising approach to the development of new supports for titania [33].

The photocatalytic properties of TiO_2 particles immobilized on Ni–TiO_2 composite electrodeposits were tested in the reaction of photochemical degradation of MB dye in water under the action of UV radia-

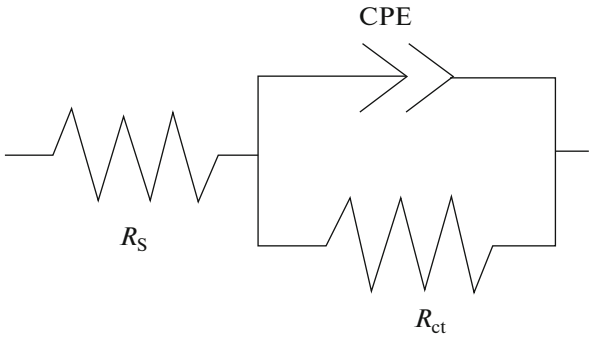

Fig. 9. Electrical equivalent circuit modeling impedance of solid electrode/solution interface.

Table 2. Calculated electrochemical impedance parameters of the corrosion of a steel substrate, Ni and Ni–TiO_2 composite coatings

System	R_s, Ω	R_{ct}, Ω cm^2	$Q \times 10^3$, Ω^{-1} s^n cm^{-2}	n
Ni	4.88	229.4	1.600	0.588
Ni–TiO_2, 1 g dm^{-3} TiO_2 in the bath	5.20	236.4	0.711	0.729
Ni–TiO_2, 2 g dm^{-3} TiO_2 in the bath	4.90	258.5	0.714	0.666
Ni–TiO_2, 5 g dm^{-3} TiO_2 in the bath	5.12	278.5	0.986	0.565
Ni–TiO_2, 10 g dm^{-3} TiO_2 in the bath	5.18	332.2	2.312	0.556
Ni–TiO_2, 15 g dm^{-3} TiO_2 in the bath	5.00	280.8	1.083	0.655
Steel substrate	4.68	128.9	3.456	0.674

tion [43]. Figure 10 gives the kinetic curves of photochemical degradation; it can be seen that they follow well the pseudo-first order kinetics. Clearly, the slopes of the straight lines plotted in the coordinates of the logarithm of the MB concentration *vs.* time allow calculating the apparent rate constants of decolorization process (Table 3).

A growth of the titania content in the plating bath and hence in the deposited composites expectedly causes the improvement in their photocatalytic performance (increasing the apparent rate constant) because of the growing of the TiO_2 photocatalyst surface concentration. After reaching some threshold value, corresponding to 10 g dm^{-3} TiO_2 in the electrolyte, the photocatalytic activity diminishes at 15 g dm^{-3} TiO_2, which may be associated with the coarsening of the surface grains and partial agglomeration of titania particles as stated above.

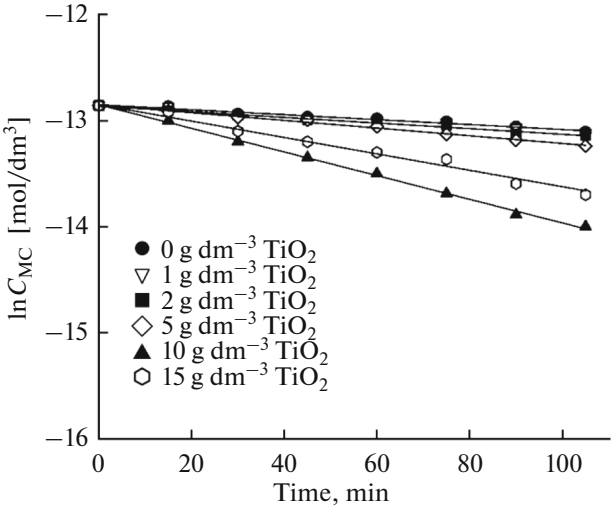

Fig 10. Kinetic curves of MB dye degradation in water under UV irradiation in the absence and in the presence of Ni–TiO_2 photocatalyst. The data are presented as first-order linear transforms ln C vs. time. Coatings were electrodeposited at stirring rate of 500 rpm, current density of 10 mA cm^{-2} and different TiO_2 contents in the plating bath.

It should be observed that there is symbasis of relationships between the investigated functional properties of coatings (their microhardness, corrosion resistance, and photocatalytic activity) and the content of TiO_2 in the plating electrolyte. All these properties reach their "best values" at a certain threshold content of the TiO_2 nano-powder in the plating bath (ca. 10 g dm^{-3}). Evidently, an extremal character of these dependences is caused by two main factors: one is related to the corresponding quantitative changes in the TiO_2 content in composite electrodeposits and the other may be connected with the observed changes of the coatings surface state (surface morphology, surface roughness, grain size, etc.).

CONCLUSIONS

(1) It is for the first time that the present work reports the main characteristics of the Ni–TiO_2 composite electrodeposition from a deep eutectic solvent, ethaline. Due to higher viscosity and density, the colloidal electrolyte based on DES ensures excellent dispersion stability as compared with "usual" aqueous systems. This is one of the most important advantages of colloidal electroplating baths containing deep eutectic solvents.

(2) The content of the titania dispersed phase in coatings depends on the TiO_2 concentration in the plating bath, the applied current density, and the stirring rate; it may reach 2.35 wt %.

(3) The Ni–TiO_2 composite electrodeposits exhibit a nano-sized type of microstructure. The introduction of titania nanoparticles into the nickel matrix affects the values of grain sizes and the surface morphology, which may be caused by changes in nucleation/growth kinetics.

(4) The co-deposition of TiO_2 particles with nickel results in an appreciable improvement in functional

Table 3. Calculated values of apparent rate constant for the reaction of MB dye degradation under UV irradiation. The coatings were electrodeposited at stirring rate of 500 rpm and current density of 10 mA cm^{-2}

Content of TiO_2 nano-powder in the plating bath, g dm^{-3}	$k \times 10^3$, min^{-1}
0 (without photocatalyst, i.e. net photolysis)	2.30
1	2.33
2	2.65
5	3.63
10	11.10
15	7.73

properties of coatings. The microhardness of composites is higher and the corrosion resistance in a corrosive medium is better than in the case of pure nickel. The incorporation of titania particles into the Ni matrix provides the coatings surface with a photocatalytic activity towards the photochemical reactions of organic dyes degradation.

(5) An increase in the TiO_2 content in composite coatings enhances microhardness, corrosion stability, and photocatalytic activity. However, after reaching a certain threshold value of the titania content, all these properties begin to weaken, probably due to more defective and less uniform surface morphology of coatings.

REFERENCES

1. Low, C.T.J., Wills, R.G.A., and Walsh, F.C., *Surf. Coat. Technol.*, 2006, vol. 201, pp. 371–383.
2. Walsh, F.C. and Ponce de Leon, C., *Trans. Inst. Met. Finish.*, 2014, vol. 92, pp. 83–98.
3. Ahmad, Y.H. and Mohamed, A.M.A., *Int. J. Electrochem. Sci.*, 2014, vol. 9, pp. 1942–1963.
4. Li, R., Hou, Y., Liu, B., Wang, D., et al., *Electrochim. Acta*, 2016, vol. 222, pp. 1272–1280.
5. Dehgahi, S., Amini, R., and Alizadeh, M., *Surf. Coat. Technol.*, 2016, vol. 304, pp. 502–511.
6. Eroglu, D. and West, A.C., *J. Electrochem. Soc.*, 2013, vol. 160, pp. D354–D360.
7. Lapinski, J., Pletcher, D., and Walsh, F.C., *Surf. Coat. Technol.*, 2011, vol. 205, pp. 5205–5209.
8. Zhang, Z., Wu, X., Jiang, C., and Ma, N., *Surf. Eng.*, 2014, vol. 30, pp. 21–25.
9. Thiemig, D. and Bund, A., *Surf. Coat. Technol.*, 2008, vol. 202, pp. 2976–2984.
10. Chen, W. and Gao, W., *Electrochim. Acta*, 2010, vol. 55, pp. 6865–6871.
11. Chen, W., He, Y., and Gao, W., *Surf. Coat. Technol.*, 2010, vol. 204, pp. 2487–2492.
12. Spanou, S., Kontos, A.I., Siokou, A., Kontos, A.G., et al., *Electrochim. Acta*, 2013, vol. 105, pp. 324–332.
13. Mohajeri, S., Dolati, A., and Ghorbani, M., *Int. J. Electrochem. Sci.*, 2017, vol. 12, pp. 5121–5141.
14. Abdel Aal, A. and Hassan, H.B., *J. Alloys Compd.*, 2009, vol. 477, pp. 652–656.
15. Mohajeri, S., Dolati, A., and Ghorbani, M., *Surf. Coat. Technol.*, 2015, vol. 262, pp. 173–183.
16. Mohan Reddy, R., Praveen, B.M., and Praveen Kumar, C.M., *Surf. Eng. Appl. Electrochem.*, 2017, vol. 53, pp. 179–185.
17. Mohan Reddy, R., Praveen, B.M., Praveen Kumar, C.M., and Venkatesha, T.V., *Surf. Eng. Appl. Electrochem.*, 2017, vol. 53, pp. 258–264.
18. Chen, X. and Mao, S.S., *Chem. Rev.*, 2007, vol. 107, pp. 2891–2959.
19. Danilov, F.I., Tsurkan, A.V., Vasil'eva, E.A., and Protsenko, V.S., *Int. J. Hydrogen Energy*, 2016, vol. 41, pp. 7363–7372.
20. Vasil'eva, E.A., Tsurkan, A.V., Protsenko, V.S., and Danilov, F.I., *Prot. Met. Phys. Chem. Surf.*, 2016, vol. 52, pp. 532–537.
21. Protsenko, V.S., Vasil'eva, E.A., Smenova, I.V., Baskevich, A.S., et al., *Surf. Eng. Appl. Electrochem.*, 2015, vol. 51, pp. 65–75.
22. Abbott, A.P., Ryder, K.S., and Konig, U., *Trans. Inst. Met. Finish.*, 2008, vol. 86, pp. 196–204.
23. Smith, E.L., Abbott, A.P., and Ryder, K.S., *Chem. Rev.*, 2014, vol. 114, pp. 11060–11082.
24. Abbott, A.P., Capper, G., Davies, D.L., Rasheed, R.K., et al., *Chem. Commun.*, 2003, vol. 1, pp. 70–71.
25. Abbott, A.P., Boothby, D., Capper, G., Davies, D.L., et al., *J. Am. Chem. Soc.*, 2004, vol. 126, pp. 9142–9147.
26. Abbott, A.P., El Ttaib, K., Frisch, G., Ryder, K.S., et al., *Phys. Chem. Chem. Phys.*, 2012, vol. 14, pp. 2443–2449.
27. Li, R., Hou, Y., and Liang, J., *Appl. Surf. Sci.*, 2016, vol. 367, pp. 449–458.
28. Li, R., Chu, Q., and Liang, J., *RSC Adv.*, 2015, vol. 5, pp. 44933–44942.
29. Abbott, A.P., El Ttaib, K., Frisch, G., McKenzie, K.J., et al., *Phys. Chem. Chem. Phys.*, 2009, vol. 11, pp. 4269–4277.
30. Pereira, N.M., Brincoveanu, O., Pantazi, A.G., Pereira, C.M., et al., *Surf. Coat. Technol.*, 2017, vol. 324, pp. 451–462.
31. Abbott, A.P., Ballantyne, A., Harris, R.C., Juma, J.A., et al., *Electrochim. Acta*, 2015, vol. 176, pp. 718–726.
32. Kityk, A.A., Shaiderov, D.A., Vasil'eva, E.A., Protsenko, V.S., and Danilov, F.I., *Electrochim. Acta*, 2017, vol. 245, pp. 133–145.
33. Protsenko, V.S., Vasil'eva, E.A., Tsurkan, A.V., Kityk, A.A., et al., *J. Environ. Chem. Eng.*, 2017, vol. 5, pp. 136–146.

34. Fransaer, J., Celis, J.P., and Roos, J.R., *J. Electrochem. Soc.*, 1992, vol. 139, pp. 413–425.

35. Maurin, G. and Lavanant, A., *J. Appl. Electrochem.*, 1995, vol. 25, pp. 1113–1121.

36. Guglielmi, N., *J. Electrochem. Soc.*, 1972, vol. 119, pp. 1009–1012.

37. Hou, F., Wang, W., and Guo, H., *Appl. Surf. Sci.*, 2006, vol. 252, pp. 3812–3817.

38. Mulder, W.H. and Sluyters, J.H., *Electrochim. Acta*, 1988, vol. 33, pp. 303–310.

39. Rammelt, U. and Reinhard, G., *Electrochim. Acta*, 1990, vol. 35, pp. 1045–1049.

40. Ranganatha, S., Venkatesha, T.V., and Vathsala, K., *Appl. Surf. Sci.*, 2010, vol. 256, pp. 7377–7383.

41. Ahmad, R., Ahmad, Z., Khan, A.U., Mastoi, N.R., et al., *J. Environ. Chem. Eng.*, 2016, vol. 4, pp. 4143–4164.

42. Shan, A.Y., Ghazi, T.I.M., and Rashid, S.A., *Appl. Catal., A*, 2010, vol. 389, pp. 1–8.

43. Houas, A., Lachheb, H., Ksibi, M., Elaloui, E., et al., *Appl. Catal., B*, 2001, vol. 31, pp. 145–157.